COMPUTER METHODS IN APPLIED MECHANICS AND ENGINEERING 60 (1987) 153–173
NORTH-HOLLAND

ON A FULLY THREE-DIMENSIONAL FINITE-STRAIN VISCOELASTIC DAMAGE MODEL: FORMULATION AND COMPUTATIONAL ASPECTS

J.C. SIMO
Applied Mechanics Division, Stanford University, Stanford, CA 94305, U.S.A.

Received 30 September 1985

A fully three-dimensional finite-strain viscoelastic model is developed, characterized by: (i) general anisotropic response, (ii) uncoupled bulk and deviatoric response over any range of deformations, (iii) general relaxation functions, and (iv) recovery of finite elasticity for very fast or very slow processes; in particular, classical models of rubber elasticity (e.g. Mooney–Rivlin). Continuum damage mechanics is employed to develop a simple isotropic damage mechanism, which incorporates softening behavior under deformation, and leads to progressive degradation of the storage modulus in a cyclic test with increasing amplitude (Mullins' effect). A numerical integration procedure is proposed which trivially satisfies objectivity and bypasses the use of midpoint configurations. The resulting algorithm can be exactly linearized in closed form, and leads to *symmetric* tangent moduli. Quasi-incompressible response is accounted for within the context of a three-field variational formulation of the Hu–Washizu type.

Introduction

A fully three-dimensional finite-strain viscoelastic constitutive model incorporating a damage mechanism is developed, based on irreversible thermodynamics with internal variables. In contrast with several formulations proposed in the past, [2, 3, 15, 30], the present approach is not restricted to isotropic response. Basic characteristics are:

(i) Local *additive decomposition of the stress tensor into initial and nonequilibrium parts*. This results from a structure of the free energy that generalizes linear viscous models.

(ii) Uncoupled volumetric and deviatoric response over any range of deformation. This is achieved by a local multiplicative decomposition of the deformation gradient into volume-preserving and dilational parts which goes back at least to Flory [12], and has been employed by Sidoroff [42], Ogden [37], Simo, Taylor and Pister [45], Lubliner [30], and Simo and Taylor [44].

(iii) Viscous response characterized by a linear rate constitutive equation, leading to a convolution representation that generalizes viscoelastic models with linearized kinematics. For relaxation times, either extremely small or very large, general finite elasticity is recovered; in particular classical models of rubber elasticity, e.g. neo-Hookean, Mooney–Rivlin, and Blatz and Ko [1].

To enhance the applicability of the model, continuum damage mechanics is employed [5, 6, 27, 28] to develop a simple three-dimensional isotropic damage mechanism. In a uniaxial test, the resulting model exhibits loss of stiffness in a range of strains lower than the previously attained maximum strain. This softening with deformation is typically observed in filled

polymers, and is often referred to as Mullins' effect [34, 47, 48]. The dependence of the stress response on the past maximum strain [10] results in the degradation of the storage moduli with increasing amplitude in a cyclic test, in agreement with experimental results [49]. Damage models based on the maximum strain concept have been often restricted to linear kinematics and one-dimensional forms [4, 17].

An essential purpose of this paper is to show that the resulting constitutive model is particularly well suited for large-scale computation. Concerning the constitutive integration algorithm it is noted that:

(iv) Generalized midpoint algorithms that ensure incremental objectivity [21, 24, 38] are entirely bypassed. The proposed integration procedure is second-order accurate and takes place entirely in the reference configuration. Incremental objectivity is trivially satisfied, and midpoint transformations are avoided.

(v) As opposed to spatial midpoint algorithms, the proposed procedure can be *exactly* linearized in closed form. Due to the structure of the rate equation characterizing inelastic response, the tangent operator is symmetric.

The overall complexity of the proposed algorithm thus compares favorably with existing computational models [18, 24], which do not even incorporate damage effects.

To appropriately account for the volume constraint emanating from a quasi-incompressible response, a mixed finite element procedure is adopted, based on a three-field variational formulation of the Hu–Washizu type, as proposed in [45]. Within this framework, widely used procedures [20, 32] can be formulated in the fully nonlinear range without resorting to rate forms. This includes interpolation schemes known to satisfy the LBB condition in the linear case [35]. In addition, iterative augmented Lagrangian procedures [13, 16] fit naturally within the present context. Consistent linearization procedures [33] are employed systematically to obtain tangent operators.

Comparison with experimental data and numerical simulations are presented to illustrate the effectiveness of the proposed formulation.

1. Nonlinear viscoelastic model

In this section we develop the basic structure of the proposed finite-strain viscoelastic model. In contrast with formulations based on a multiplicative decomposition of the deformation gradient [15, 30, 42] or on an additive split of the Lagrangian strain tensor [7], the proposed model results in an additive split of the stress tensor into *initial and nonequilibrium* parts. However, for the particular case of neo-Hookean type of elastic response, the model is consistent with a multiplicative decomposition of the deformation gradient. The assumption of isotropy, crucial in the Green and Tobolsky model and its subsequent extension due to Lubliner [30], is not invoked here. Furthermore, as opposed to second-order theories based on asymptotic expansions [7], complete uncoupling over any range of strains of volumetric and deviatoric responses may be obtained due to the exact multiplicative split into volume-preserving and dilational parts discussed below.

1.1. Motivation. Linear theory

To motivate the fully nonlinear formulation developed below, we first consider the following alternative formulation of the standard linear solid. Let $\Psi(\varepsilon, q)$ be the free energy

defined as

$$\Psi(\varepsilon, q) := U^0(\operatorname{tr}\varepsilon) + \bar{\Psi}^0(e) - q : e + \Psi_I(q) . \tag{1.1}$$

Here, U^0 and $\bar{\Psi}^0$ are the volumetric and deviatoric parts of the initial elastic stored energy function Ψ^0 (uncoupling is assumed), and $e = \operatorname{dev}[\varepsilon]$ is the strain deviator, where $\operatorname{dev}[\cdot] = (\cdot) - \frac{1}{3}\operatorname{tr}(\cdot)\mathbf{1}$. For the isotropic case one has $U^0(\operatorname{tr}\varepsilon) = \frac{1}{2}K^0(\operatorname{tr}\varepsilon)^2$ and $\bar{\Psi}^0(e) = \mu^0\|e\|^2$. In the present formulation q is an internal variable governed by the following equation of evolution:

$$\dot{q} + \frac{1}{\nu} q = \frac{1-\gamma}{\nu} \operatorname{dev}[\partial\bar{\Psi}^0(e)/\partial e] , \quad q|_{t=0} = \mathbf{0} , \tag{1.2}$$

where $\gamma \in [0, 1)$ is a given parameter. Note that for the standard solid $(1-\gamma)q/\gamma$ gives the (nonequilibrium) force acting on the spring parallel to the dashpot. The second law of thermodynamics gives

$$\sigma = \partial\Psi(\varepsilon, q)/\partial\varepsilon \equiv \sigma^0 - q , \tag{1.3}$$

where $\sigma^0 := \partial\Psi^0(\varepsilon)/\partial\varepsilon$. Thus, we have an additive decomposition of the current stress tensor into initial stress σ^0 and nonequilibrium stress q. Integration of (1.2) and substitution of q into (1.3) yield the classical convolution representation of the standard linear solid.

REMARK 1.1. $\Psi_I(q)$ in (1.1) is determined from the conditions of thermodynamic equilibrium. As an example, assuming rate equation (1.2), at equilibrium $\partial\Psi(\varepsilon, q)/\partial q = 0$ and $\dot{q} = 0$, so that from (1.1) and (1.2) one has

$$e = \partial\Psi_I(q)/\partial q \quad \text{and} \quad q = (1-\gamma)\operatorname{dev}[\partial\bar{\Psi}^0(e)/\partial e] . \tag{1.4}$$

It follows from (1.4) that $\Psi_I(q)$ is given by the Legendre transformation

$$\Psi_I(q) = -(1-\gamma)\bar{\Psi}^0(e) + e : q . \tag{1.5}$$

Note that for the isotropic case $\Psi_I(q) = (1/4\mu^0(1-\gamma))\|q\|^2$.

The formulation outlined can be extended to the fully nonlinear case as follows.

1.2. Kinematic split and structure of the free energy

Let $\varphi(X, t): B \times \mathbb{R} \to \mathbb{R}^3$ denote the motion and let $F(X, t)$ be the deformation gradient. Here $X \in \mathbb{R}^3$ designates the position of a particle in the reference configuration $\Omega \subset \mathbb{R}^3$. Further, let $J \equiv \det F$ be the Jacobian of the deformation gradient. To properly define volumetric and deviatoric reponses in the nonlinear range, we introduce the following kinematic split:

$$F = J^{1/3}\bar{F} \quad \text{where} \quad \bar{F} := J^{-1/3}F , \qquad F := \partial\Phi/\partial X . \tag{1.6}$$

Since $\det\bar{F} \equiv 1$, we refer to $\bar{F}$ as the *volume-preserving part* of the deformation gradient F.

Associated with $\boldsymbol{F}$ and $\bar{\boldsymbol{F}}$ we define the corresponding right Cauchy–Green tensors as

$$\boldsymbol{C} = \boldsymbol{F}^{\mathrm{t}}\boldsymbol{F}\,, \qquad \bar{\boldsymbol{C}} = J^{-2/3}\boldsymbol{C} \equiv \bar{\boldsymbol{F}}^{\mathrm{t}}\bar{\boldsymbol{F}}\,. \tag{1.7a,b}$$

Lagrangian strain tensors are given by the standard expressions

$$\boldsymbol{E} := \tfrac{1}{2}[\boldsymbol{C} - \boldsymbol{G}]\,, \qquad \bar{\boldsymbol{E}} := \tfrac{1}{2}[\bar{\boldsymbol{C}} - \boldsymbol{G}]\,, \tag{1.8}$$

where $\boldsymbol{G}$ is the metric tensor in the reference configuration (in Cartesian components, $G_{IJ} \equiv \delta_{IJ}$).

REMARK 1.2. Expression (1.7b) furnishes the proper generalization to finite motions of the decomposition of the linearized strain tensor into spherical and deviatoric parts. To illustrate the point consider the linearization of (1.7b) about $\varphi \equiv$ Identity. Let $\varphi_\varepsilon \equiv \varphi + \varepsilon \boldsymbol{u} \circ \varphi$, where $\varepsilon \in \mathbb{R}$, and $\boldsymbol{u}: \varphi(\Omega) \to \mathbb{R}^3$ is an incremental displacement from $\varphi(\Omega)$. Since $\boldsymbol{F}_\varepsilon = [\boldsymbol{F} + \varepsilon \nabla \boldsymbol{u}\boldsymbol{F}]$ and $\boldsymbol{C}_\varepsilon \equiv \boldsymbol{F}_\varepsilon^{\mathrm{t}}\boldsymbol{F}_\varepsilon$, it follows that

$$\frac{\mathrm{d}}{\mathrm{d}\varepsilon}\bigg|_{\varepsilon=0} \det \boldsymbol{F}_\varepsilon = (\det \boldsymbol{F})\,\mathrm{tr}\,\nabla \boldsymbol{u} \;\Rightarrow\; \frac{\mathrm{d}}{\mathrm{d}\varepsilon}\bigg|_{\varepsilon=0} \boldsymbol{C}_\varepsilon = \boldsymbol{F}^{\mathrm{t}}(\nabla^{\mathrm{t}}\boldsymbol{u} + \nabla \boldsymbol{u})\boldsymbol{F}\,. \tag{1.9}$$

Since $\boldsymbol{F} \equiv \boldsymbol{1}$ at $\varphi =$ Identity, the linearization of (1.7b) yields the relation $\boldsymbol{e} = \boldsymbol{\varepsilon} - \frac{1}{3}(\mathrm{tr}\,\nabla \boldsymbol{u})\boldsymbol{1}$ of the linear theory.

Motivated by (1.1) for the linear theory, we postulate an uncoupled free energy function $\boldsymbol{\Psi}(\boldsymbol{E}, \boldsymbol{Q})$ of the form[1]

$$\boldsymbol{\Psi}(\boldsymbol{E}, \boldsymbol{Q}) := U^0(J) + \bar{\boldsymbol{\Psi}}^0(\bar{\boldsymbol{E}}) - \boldsymbol{Q} : \bar{\boldsymbol{E}} + \boldsymbol{\Psi}_I(\boldsymbol{Q})\,, \tag{1.10}$$

where $\boldsymbol{Q}$ plays the role of an internal variable. Let $\boldsymbol{\tau} = J\boldsymbol{\sigma} = \boldsymbol{F}\boldsymbol{S}\boldsymbol{F}^{\mathrm{t}}$ denote the Kirchhoff stress tensor, where $\boldsymbol{\sigma}$ is the Cauchy stress tensor, and $\boldsymbol{S}$ is the symmetric Piola–Kirchoff stress tensor. Restricting our attention to the isothermal case, standard arguments [9], exploiting the Clausius–Duhem inequality $-\dot{\boldsymbol{\Psi}} + \frac{1}{2}\boldsymbol{S} : \dot{\boldsymbol{C}} \geq 0$, lead to

$$-\frac{\partial \boldsymbol{\Psi}(\boldsymbol{E}, \boldsymbol{Q})}{\partial \boldsymbol{Q}} : \dot{\boldsymbol{Q}} \geq 0\,, \qquad \boldsymbol{S} = \frac{\partial \boldsymbol{\Psi}(\boldsymbol{E}, \boldsymbol{Q})}{\partial \boldsymbol{E}}\,. \tag{1.11}$$

Straightforward application of the chain rule along with the formula $\partial J/\partial \boldsymbol{C} = J/2\boldsymbol{C}^{-1}$ yields

$$\partial \bar{\boldsymbol{E}}/\partial \boldsymbol{E} \equiv \partial \bar{\boldsymbol{C}}/\partial \boldsymbol{C} \equiv J^{-2/3}[\boldsymbol{I} - \tfrac{1}{3}\boldsymbol{C} \otimes \boldsymbol{C}^{-1}]\,, \tag{1.12}$$

where $\boldsymbol{I}$ is the symmetric rank-four unit tensor. From (1.10)–(1.12) we obtain the following constitutive equation for the second Piola–Kirchhoff tensor:

[1]There is no difficulty in considering forms other than (1.10). Typically, elastic stored energy functions of the form $\boldsymbol{\Psi} := J\bar{\boldsymbol{\Psi}}^0(\boldsymbol{E}) + U^0(J)$ may be more appropriate for rubberlike materials [36].

$$\boldsymbol{S} = Jp\boldsymbol{C}^{-1} + J^{-2/3}\mathrm{DEV}[\partial\bar{\boldsymbol{\Psi}}^0(\bar{\boldsymbol{E}})/\partial\bar{\boldsymbol{E}} - \boldsymbol{Q}]\,. \tag{1.13a}$$

Here $p \equiv \mathrm{d}U^0(J)/\mathrm{d}J$ denotes the hydrostatic pressure and $\mathrm{DEV}[\cdot]: = (\cdot) - \frac{1}{3}[\boldsymbol{C}:(\cdot)]\boldsymbol{C}^{-1}$. Note that $\mathrm{DEV}[\cdot]$ gives the physically correct deviator in the reference configuration, with the right Cauchy–Green tensor $\boldsymbol{C}$ operating as metric tensor. Since $\boldsymbol{\tau} = \boldsymbol{F}\boldsymbol{S}\boldsymbol{F}^t$, in the spatial description expression (1.13a) may be recast in the equivalent form

$$\boldsymbol{\tau} = Jp\mathbf{1} + \mathrm{dev}[\bar{\boldsymbol{F}}\{\partial\bar{\boldsymbol{\Psi}}^0(\bar{\boldsymbol{E}})/\partial\bar{\boldsymbol{E}} - \boldsymbol{Q}\}\bar{\boldsymbol{F}}^t]\,, \tag{1.13b}$$

where $\mathrm{dev}[\cdot] \equiv (\cdot) - \frac{1}{3}\,\mathrm{tr}(\cdot)\mathbf{1}$ denotes the deviator (in the spatial configuration) of the indicated argument.

EXAMPLE 1.3. An example of the elastic constitutive equation is furnished by the following *uncoupled* stored energy function:

$$\boldsymbol{\Psi}^0(\boldsymbol{E}) = \tfrac{1}{2}\mu^0\bar{I} + U^0(J)\,, \tag{1.14}$$

where $\bar{I}: = \mathrm{tr}\,\bar{\boldsymbol{b}}$ is the first invariant of $\bar{\boldsymbol{b}} \equiv \bar{\boldsymbol{F}}\bar{\boldsymbol{F}}^t$ and $\mu^0 > 0$ is a constant (shear modulus). It follows from (1.13a, b) that the Kirchhoff and symmetric Piola–Kirchhoff tensors are given by

$$\boldsymbol{\tau} \equiv Jp\mathbf{1} + \mu^0\,\mathrm{dev}[\bar{\boldsymbol{b}} - \bar{\boldsymbol{F}}\boldsymbol{Q}\bar{\boldsymbol{F}}^t]\,, \qquad \boldsymbol{S} = Jp\boldsymbol{C}^{-1} + \mu^0 J^{-2/3}\,\mathrm{DEV}[\boldsymbol{G} - \boldsymbol{Q}]\,, \tag{1.15}$$

where $\mathrm{DEV}[\boldsymbol{G}] = \boldsymbol{G} - \frac{1}{3}(\boldsymbol{G}:\boldsymbol{C})\boldsymbol{C}^{-1}$. This model furnishes an extension to the compressible range of the classical neo-Hookean model and was employed by Simo et al. [45] for finite deformation elastoplasticity formulated in the context of a multiplicative decomposition.

1.3. *Rate equation and convolution representation*

Motivated by our discussion of Section 1.1, we propose the following *linear* rate equation to introduce "standard solid" type of viscoelastic behavior:

$$\dot{\boldsymbol{Q}} + \frac{1}{\nu}\boldsymbol{Q} = \frac{(1-\gamma)}{\nu}\,\mathrm{DEV}\left[\frac{\partial\bar{\boldsymbol{\Psi}}^0(\bar{\boldsymbol{E}})}{\partial\bar{\boldsymbol{E}}}\right], \quad \boldsymbol{Q}|_{t=0} = 0\,, \tag{1.16}$$

where $\nu \in [0, \infty)$ is the relaxation time and $\gamma \in [0, 1)$ is given parameter. As in Section 1.1., the linear structure of (1.16) enables us to express $\boldsymbol{Q}$ in terms of a simple convolution integral. Substitution into (1.13a) and (1.13b) then yields the following equivalent expressions in terms of either the Kirchhoff or the symmetric Piola–Kirchhoff tensors,

$$\begin{aligned}
&\boldsymbol{S} = Jp\boldsymbol{C}^{-1} + J^{-2/3}\,\mathrm{DEV}[\boldsymbol{H}] \;\Rightarrow\; \boldsymbol{\tau} = Jp\mathbf{1} + \mathrm{dev}[\bar{\boldsymbol{F}}\boldsymbol{H}\bar{\boldsymbol{F}}^t]\,,\\
&\boldsymbol{H}: = \int_0^t (\gamma + (1-\gamma)\,\mathrm{e}^{(-(t-s)/\nu)})\,\frac{\mathrm{d}}{\mathrm{d}s}\left\{\mathrm{DEV}\left[\frac{\partial\bar{\boldsymbol{\Psi}}^0(\bar{\boldsymbol{E}}(s))}{\partial\bar{\boldsymbol{E}}}\right]\right\}\mathrm{d}s\,,\\
&\mathrm{DEV}[\cdot]: = (\cdot) - \tfrac{1}{3}[(\cdot):\boldsymbol{C}]\boldsymbol{C}^{-1}\,.
\end{aligned} \tag{1.17}$$

We note the following.

REMARK 1.4. $\gamma = 0$ corresponds to a Maxwell fluid, whereas $\gamma = 1$ defines an elastic solid. Any model of linear viscoelasticity may be trivially considered by an appropriate choice of the kernel in the convolution representation for $\boldsymbol{H}$. As an example, several relaxation times may be introduced by replacing the single term $\gamma + (1-\gamma)\exp[-t/\nu]$ with the kernel

$$K(t) := \gamma_0 + \sum_{\alpha=1}^{N} \gamma_\alpha \, e^{-t/\nu_\alpha} . \tag{1.18}$$

A continuous spectrum of relaxation times could also be introduced [8]. Similarly, $\boldsymbol{H}$ in (1.17) may also be defined by convolution representations involving fractional derivatives [25, 40], or power type of kernels as in [29].

REMARK 1.5. Equilibrium. The conditions of thermodynamic equilibrium are given by

$$\partial \boldsymbol{\Psi}(\boldsymbol{E}, \boldsymbol{Q}) / \partial \boldsymbol{Q} \equiv -\bar{\boldsymbol{E}} + \partial \boldsymbol{\Psi}_I(\boldsymbol{Q}) / \partial \boldsymbol{Q} = \boldsymbol{0} , \qquad \boldsymbol{Q} = (1-\gamma)\,\mathrm{DEV}[\partial \bar{\boldsymbol{\Psi}}^0(\bar{\boldsymbol{E}}) / \partial \bar{\boldsymbol{E}}] . \tag{1.19}$$

Note that $\boldsymbol{Q}$ attains its equilibrium value as $t/\nu \to \infty$. The corresponding value of the equilibrium stress is a fraction γ of the initial stress; that is

$$\lim_{t/\nu \to \infty} \boldsymbol{S} = \{ Jp\boldsymbol{C}^{-1} + \gamma J^{-2/3}\,\mathrm{DEV}[\partial \bar{\boldsymbol{\Psi}}^0(\bar{\boldsymbol{E}}) / \partial \bar{\boldsymbol{E}}] \} =: Jp\boldsymbol{C}^{-1} + \gamma\,\mathrm{DEV}[\boldsymbol{S}^0] . \tag{1.20}$$

Since $\boldsymbol{S} \equiv \boldsymbol{S}^0$ as $t/\nu \to 0$, we conclude that finite elasticity is recovered for both very slow and very fast processes. We finally note that, as in the linear theory, conditions (1.19) show that the function $\boldsymbol{\Psi}_I(\boldsymbol{Q})$ is given by the Legendre transformation

$$\boldsymbol{\Psi}_I(\boldsymbol{Q}) = -(1-\gamma)\bar{\boldsymbol{\Psi}}^0(\bar{\boldsymbol{E}}) + \bar{\boldsymbol{E}} : \boldsymbol{Q} . \tag{1.21}$$

REMARK 1.6. For the particular elastic response given in Example 1.3 (compressible neo-Hookean), it can be shown that model (1.17) is consistent with a multiplicative decomposition of the deformation gradient of the form $\boldsymbol{F} = \boldsymbol{F}_e \boldsymbol{F}_i$, with internal variable $\boldsymbol{Q} \equiv \mu^0 \boldsymbol{C}_i^{-1}$, and $\boldsymbol{C}_i^{-1} := \boldsymbol{F}_i^{-1} \boldsymbol{F}_i^{-t}$. The resulting model is similar to the class of isotropic models proposed by Lubliner [30] as an extension of the Green and Tobolsky model [15]. Note, however, that even in this case rate equation (1.16) differs from that proposed in [30]. It can be shown that, in contrast with (1.16), the latter equation results in a *nonsymmetric* tangent operator.

We finally note that model (1.17) fits within the notion of "simple material" in the sense of Noll [46, Section 29, equation (29.6)].

2. Phenomenological isotropic damage model

Material damage in polymers is a complex process which may involve chain and multichain damage, microstructural damage, and microvoid formation [14, 26]. Here, our purpose is to account for the loss of stiffness experimentally observed in polymers when subjected to levels

of strain below the maximum strain previously attained by the specimen. This softening of rubber by deformation is commonly referred to as "Mullins' effect" [34, 47–49]. Typically, the uniaxial stress-strain curve remains insensitive at strains above the previous maximum, but experiences a substantial softening below this maximum strain. The higher the previously attained maximum the bigger the subsequent loss of stiffness. In a cyclic test, this effect results in a progressive reduction of the storage moduli with increasing maximum strain amplitude. Almost all of the loss in stiffness takes place at first deformation, and steady-state response is attained in very few cycles provided the maximum strain amplitude remains constant.

In what follows a phenomenological point of view is adopted, based on the use of continuous damage mechanics and the "equivalent stress" concept first introduced by Kachanov [22]. See, e.g., [5, 6, 27, 28]. Within this framework, a simple three-dimensional isotropic damage mechanism is developed, which is suitable for computation. The crucial assumption is that the *maximum strain* attained by the specimen up to the present time completely controls the damage process [4, 10, 17]. Based on thermodynamic arguments, we generalize this notion to the 3-D case by introducing the strain energy of the undamaged material as a scalar measure of the maximum strain. This choice is essential from a computational standpoint, since it results in a symmetric tangent stiffness. Two example models are considered.

2.1. Motivation. Elastic damage at finite strains

We consider first the case of a material initially characterized by a general stored energy function $\boldsymbol{\Psi}^0(\boldsymbol{E})$ undergoing an isotropic damage process. The point of departure is a free energy of the form

$$\boldsymbol{\Psi}(\boldsymbol{E}, D) = (1 - D)\boldsymbol{\Psi}^0(\boldsymbol{E}), \tag{2.1}$$

where $D \in [0, 1]$ is the damage parameter and $(1 - D)$ a reduction factor of the form first suggested by Kachanov [22]. From the Clausius–Duhem inequality $-\dot{\boldsymbol{\Psi}} + \boldsymbol{S} : \dot{\boldsymbol{E}} > 0$, it follows that

$$-\frac{\partial \boldsymbol{\Psi}(\boldsymbol{E}, D)}{\partial D}\dot{D} \equiv \boldsymbol{\Psi}^0(\boldsymbol{E})\dot{D} \geq 0, \qquad \boldsymbol{S} = (1 - D)\frac{\partial \boldsymbol{\Psi}^0(\boldsymbol{E})}{\partial \boldsymbol{E}}. \tag{2.2a, b}$$

Inequality (2.2a) expresses the fact that damage is a dissipative process. Constitutive equation (2.2b), on the other hand, is the finite-strain version of the equivalent stress concept first introduced by Kachanov [22].

2.1.1. Evolution of damage

We first note that the "elastic" stored energy function of the undamaged material, $\boldsymbol{\Psi}^0(\boldsymbol{E})$, is the thermodynamic variable conjugate to the damage variable D, since $\partial \boldsymbol{\Psi}/\partial D \equiv -\boldsymbol{\Psi}^0(\boldsymbol{E})$. The evolution of the damage parameter D is then characterized by an *irreversible* equation of evolution as follows. Define an equivalent strain Ξ_s by the expression

$$\Xi_s := \sqrt{2\boldsymbol{\Psi}^0(\boldsymbol{E}(s))}, \tag{2.3}$$

where $\boldsymbol{E}(s)$ is the strain tensor at time $s \in \mathbb{R}_+$. Now, let Ξ_t^m be the maximum value of Ξ_s over

the past history up to current time $t \in \mathbb{R}_+$. That is,

$$\Xi_t^{\mathrm{m}} := \max_{s \in (-\infty, t]} \sqrt{2\Psi^0(E(s))}\,. \tag{2.4}$$

We define a *damage criterion* in strain space by the condition that at any time $t \in \mathbb{R}_+$ of the loading process,

$$\varphi(E(t), \Xi_s^{\mathrm{m}}) := \sqrt{2\Psi^0(E(t))} - \Xi_t^{\mathrm{m}} \leq 0\,. \tag{2.5}$$

The equation $\varphi(E(t), \Xi_t^{\mathrm{m}}) = 0$ defines a damage surface in the strain space. Denoting by $N := \partial\varphi/\partial E \equiv (1/\Xi_s)\,\partial\Psi^0/\partial E$, the normal to the damage surface, the following alternative situations may occur: either

$$\varphi < 0 \quad \text{or} \quad \varphi = 0 \quad \text{and} \quad \begin{cases} N : \dot{E} < 0\,, \\ N : \dot{E} = 0\,, \\ N : \dot{E} > 0\,. \end{cases} \tag{2.6}$$

Borrowing a terminology typically found in (strain space) plasticity [31], we speak of unloading, neutral loading, or loading from a damage state, according to the sign of $N : \dot{E}$. Finally, the evolution of the damage variable D is specified by the irreversible rate equation

$$\frac{\mathrm{d}D}{\mathrm{d}t} = \begin{cases} \bar{h}(\Xi, D)\dot{\Xi}\,, & \text{if } \varphi = 0 \text{ and } N : \dot{E} > 0\,, \\ 0\,, & \text{otherwise}\,. \end{cases} \tag{2.7}$$

Here $\bar{h}(\Xi, D)$ is a given function that characterizes the damage process in the material. This completes the formulation of the elastic-damage model at finite strains. Regarding this formulation the following should be noted.

REMARK 2.1. If $\bar{h}(\Xi, D)$ in (2.7) is *independent* of D, then the isotropic damage model outlined above may be expressed in the following equivalent form:

$$S(t) = \bar{g}(\Xi_t^{\mathrm{m}})\,\partial\Psi^0(E(t))/\partial E \quad \text{where} \quad \Xi_t^{\mathrm{m}} := \max_{s \in (-\infty, t]} \sqrt{2\Psi^0(E(s))}\,. \tag{2.8}$$

This form follows simply by setting $\bar{h}(\Xi) = -\mathrm{d}\bar{g}(\Xi)/\mathrm{d}\Xi$. One-dimensional models with the stress tensor depending on the maximum value attained by the stress during the loading history have been proposed by Browning, Gurtin and Williams [4], Gurtin and Francis [17], and Simo and Taylor [43, 44].

REMARK 2.2. We note that the evolution of the stress tensor is completely determined. Employing the notation of Remark 2.1 and making use of the chain rule we have

$$\dot{S}(s) = \begin{cases} \left[\bar{g}(\Xi^{\mathrm{m}}_t) \dfrac{\partial^2 \Psi^0}{\partial E^2} + \dfrac{\bar{g}'(\Xi^{\mathrm{m}})}{\Xi^{\mathrm{m}}} \dfrac{\partial \Psi^0}{\partial E} \otimes \dfrac{\partial \Psi^0}{\partial E} \right] : \dot{E} , & \text{iff } \varphi = 0 \text{ and } N : \dot{E} > 0 , \\ \bar{g}(\Xi^{\mathrm{m}}_t) \dfrac{\partial^2 \Psi^0}{\partial E^2} : \dot{E} , & \text{otherwise} , \end{cases} \tag{2.9}$$

where $\bar{g}' := \mathrm{d}\bar{g}/\mathrm{d}\Xi \equiv -\bar{h}$. In what follows, attention is restricted to this case.

REMARKS 2.3. To completely determine the damage model, it remains to specify the function $\bar{g}(\Xi^{\mathrm{m}})$ in (2.8) or, equivalently, the function $\bar{h} = -\mathrm{d}\bar{g}/\mathrm{d}\Xi$ in (2.7). Such a determination should be made on the basis of available experimental data. Here, for definiteness, we shall adopt the following exponential form [43, 44]:

$$\bar{g}(x) = \beta + (1 - \beta) \frac{1 - \mathrm{e}^{-x/\alpha}}{x/\alpha} , \quad \beta \in [0, 1] , \ \alpha \in [0, \infty) . \tag{2.10}$$

In this relationship, β and α are regarded as given parameters.

2.2. Viscoelastic damage model

The ideas discussed above can be readily extended to account for viscous effects by the same approach of Section 1. Employing the notation of Remark 2.1, the elastic-damage free energy (2.1) is replaced by the augmented free energy

$$\Psi(E, Q, \Xi^{\mathrm{m}}) := \bar{g}(\Xi^{\mathrm{m}}) \Psi^0(E) - Q : E + \Psi_I(Q) . \tag{2.11}$$

Standard arguments based on the Clausius–Duhem inequality lead to the representation

$$S = \bar{g}(\Xi^{\mathrm{m}}) \frac{\partial \Psi^0(E)}{\partial E} - Q . \tag{2.12}$$

Finally, the evolution of the internal variable Q, which represents the nonequilibrium viscous stress, may be specified by a linear rate equation. For the standard solid, for instance, one has (1.16) with the right-hand side now given by $((1 - \gamma)/\nu)\bar{g}(\Xi^{\mathrm{m}}_s)\, \partial \Psi^0(E)/\partial E$. As a result one obtains the convolution model

$$S = \int_0^t K(t - s) \frac{\mathrm{d}}{\mathrm{d}s} \left[\bar{g}(\Xi_s) \frac{\partial \Psi^0}{\partial E} (E(s)) \right] \mathrm{d}s , \tag{2.13}$$

where $K(t)$ is the relaxation function. In this expression, volumetric and deviatoric effects are not uncoupled, an assumption often made in viscoelastic analysis. To incorporate this feature into the model, we may proceed as in Section 1. Two examples of this type are summarized below.

EXAMPLE 2.4. The following example assumes uncoupled volumetric/deviatoric response.

In addition, we assume that the damage mechanism is associated with maximum distortional energy and is independent of hydrostatic pressure.

$$
\begin{aligned}
&\boldsymbol{\tau} = Jp\mathbf{1} + \operatorname{dev}[\bar{\boldsymbol{F}}\boldsymbol{H}\bar{\boldsymbol{F}}^{t}] ,\\
&\boldsymbol{H} := \int_0^t K(t-s)\,\frac{\mathrm{d}}{\mathrm{d}s}\,[\boldsymbol{\Pi}(\bar{\boldsymbol{E}}(s), \Xi^{m}_{s})]\,\mathrm{d}s ,\\
&\boldsymbol{\Pi}(\bar{\boldsymbol{E}}(s), \Xi^{m}_{s}) := \bar{g}(\Xi^{m}_{s})\,\operatorname{DEV}[\partial\bar{\boldsymbol{\Psi}}^{0}(\bar{\boldsymbol{E}}(s))/\partial\bar{\boldsymbol{E}}] ,\\
&\Xi^{m}_{t} := \max_{s\in(-\infty,\,t]} \sqrt{2\bar{\boldsymbol{\Psi}}^{0}(\bar{\boldsymbol{E}}(s))} ,\\
&\bar{g}(x) = \beta + (1-\beta)\,\frac{1-\mathrm{e}^{-x/\alpha}}{x/\alpha} , \quad \beta\in[0,1] , \ \alpha\in[0,\infty) .
\end{aligned}
\tag{2.14}
$$

For the compressible case we have that $p = \mathrm{d}U^{0}(J)/\mathrm{d}J$. Note that there is no difficulty in including the effect of hydrostatic pressure by replacing $\bar{\boldsymbol{\Psi}}^{0}$ with $\bar{\boldsymbol{\Psi}}^{0} + U^{0}$ in the definition of Ξ^{m}_{t}, as in (2.12). However, this results in nonsymmetric algorithmic tangent moduli.

EXAMPLE 2.5. Different theories and damage mechanisms warrant different definitions of Ξ^{m}_{t} and a different expression of the free energy. For instance, it has been suggested that the degree of damage in polymers is a function of the hydrostatic pressure (e.g. [40, p. 167]). Assuming an uncoupled volumetric/deviatoric response, a possible finite-strain viscoelastic damage model incorporating this mechanism is given by (1.17) with the hydrostatic pressure now defined as follows:

$$
\begin{aligned}
&\boldsymbol{\tau} = J\tilde{p}\mathbf{1} + \operatorname{dev}\left[\bar{\boldsymbol{F}}\left\{\int_0^t K(t-s)\,\frac{\mathrm{d}}{\mathrm{d}s}\,\operatorname{DEV}[\partial\bar{\boldsymbol{\Psi}}^{0}(\bar{\boldsymbol{E}}(s))/\partial\bar{\boldsymbol{E}}]\,\mathrm{d}s\right\}\bar{\boldsymbol{F}}^{t}\right] ,\\
&\tilde{p} := \bar{g}(\tilde{\Xi}^{m})\,\mathrm{d}U^{0}(J)/\mathrm{d}J , \qquad \tilde{\Xi}^{m}_{t} := \max_{s\in(-\infty,\,t)} \sqrt{2U^{0}(J(S))} .
\end{aligned}
\tag{2.15}
$$

We note that this model results from a free energy potential of the form

$$
\boldsymbol{\Psi}(\boldsymbol{E}, \boldsymbol{Q}, \tilde{\Xi}^{m}) := \bar{g}(\tilde{\Xi})U^{0}(J) + \bar{\boldsymbol{\Psi}}^{0}(\bar{\boldsymbol{E}}) - \boldsymbol{Q}:\bar{\boldsymbol{E}} + \boldsymbol{\Psi}_{I}(\boldsymbol{Q}) .
\tag{2.16}
$$

As shown in Section 3, both this model and model (2.14) lead to algorithmic tangent moduli which are symmetric.

3. Integration algorithm for constitutive equations

The basic idea in the numerical integration of constitutive equations (1.9) and (1.12) is to evaluate the convolution integral in (1.12) through a recurrence relation. A related procedure was first suggested by Herrmann and Peterson [19], and employed by Key and Krieg [24] in a finite-strain context. However, the crucial difference with the latter approach is that the need for an incrementally objective algorithm based on the use of a midpoint configuration, as

proposed by Hughes and Winget [21], is entirely bypassed. As a result, intermediate midpoint transformations employing half-increment rotation tensors are avoided. In addition, by contrast with midpoint algorithms, the proposed approach can be exactly linearized in closed form.

Without loss of generality we shall consider standard solid viscoelasticity and the constitutive model of Example 2.4. Identical considerations apply to Example 2.5. Let $[0, T] \subset \mathbb{R}$ be the time interval of interest. We introduce the following history variable $\bar{\boldsymbol{H}}(t_n)$ defined at any time $t_n \in [0, T]$ by

$$\bar{\boldsymbol{H}}(t_n) := \int_0^{t_n} \mathrm{e}^{-(t_n - s)/\nu}\, \dot{\boldsymbol{\Pi}}(\bar{\boldsymbol{E}}(s), \Xi^{\mathrm{m}}_s)\, \mathrm{d}s\,. \tag{3.1}$$

Then we proceed to update the stress tensor as follows. It is essential to recall that from a computational standpoint this update process is always regarded as *strain driven*.

3.1. Recursive update of the stress deviator at Gauss points

Let $\boldsymbol{x}_n \equiv \varphi_n(\boldsymbol{X}, t_n)$ be the configuration at time t_n, assumed to be known. Further, let an incremental displacement field $\boldsymbol{U}(\boldsymbol{X}) \equiv \boldsymbol{u}(\varphi_n(\boldsymbol{X}, t_n))$ be given. Since the process is strain driven, we simply set

$$\varphi_{n+1} = \varphi_n + \boldsymbol{U}\,, \qquad \boldsymbol{F}_{n+1} = \boldsymbol{F}_n + \mathrm{GRAD}\,\boldsymbol{U} \equiv [\mathbf{1} + \nabla_n \boldsymbol{u}]\boldsymbol{F}_n\,, \qquad \boldsymbol{C}_{n+1} := \boldsymbol{F}^{\mathrm{t}}_{n+1}\boldsymbol{F}_{n+1}\,, \tag{3.2}$$

where $\mathrm{GRAD}\,(\cdot)$ is the gradient relative to $\boldsymbol{X} \in \Omega$, and $\nabla_n(\cdot)$ is the gradient relative to $\boldsymbol{x}_n$. From (3.2) we immediately have

$$\bar{\boldsymbol{F}}_{n+1} := (\det \boldsymbol{F}_{n+1})^{-1/3}\boldsymbol{F}_{n+1}\,, \qquad \bar{\boldsymbol{C}}_{n+1} := \bar{\boldsymbol{F}}^{\mathrm{t}}_{n+1}\bar{\boldsymbol{F}}_{n+1}\,, \qquad \bar{\boldsymbol{E}}_{n+1} := \tfrac{1}{2}[\bar{\boldsymbol{C}}_{n+1} - \boldsymbol{G}]\,. \tag{3.3}$$

Next, the evolution of damage is evaluated as follows. The damage variable Ξ^{m}_{n+1} is updated as

$$\Xi^{\mathrm{m}}_{n+1} := \max\{\Xi^{\mathrm{trial}}_{n+1}, \Xi_n\} \quad \text{where} \quad \Xi^{\mathrm{trial}}_{n+1} := \sqrt{2\bar{\Psi}^0(\bar{\boldsymbol{E}}_{n+1})}\,. \tag{3.4a}$$

Then $\boldsymbol{\Pi}_{n+1}$ is computed as

$$\boldsymbol{\Pi}_{n+1} = \bar{g}(\Xi^{\mathrm{m}}_{n+1})\,\mathrm{DEV}_{n+1}\left[\frac{\partial \bar{\Psi}^0}{\partial \bar{\boldsymbol{E}}}\,(\bar{\boldsymbol{E}}_{n+1})\right], \tag{3.4b}$$

where

$$\mathrm{DEV}_{n+1}[\,\cdot\,] := (\,\cdot\,) - \tfrac{1}{3}[(\,\cdot\,) : \boldsymbol{C}_{n+1}]\boldsymbol{C}^{-1}_{n+1}\,. \tag{3.4c}$$

To update $\bar{\boldsymbol{H}}_n$, defined by (3.1), use is made of the midpoint rule and the mean value theorem to obtain the following expression

$$\bar{\boldsymbol{H}}_{n+1} = \mathrm{e}^{-\Delta t_n/\nu}\,\bar{\boldsymbol{H}}_n + \frac{1 - \mathrm{e}^{-\Delta t_n/\nu}}{\Delta t_n/\nu}\,[\boldsymbol{\Pi}_{n+1} - \boldsymbol{\Pi}_n]\,. \tag{3.5}$$

The deviator of the second Piola–Kirchhoff stress tensor S_n is then updated according to

$$\mathrm{DEV}_{n+1}[S_{n+1}] \equiv (\det F_{n+1})^{-2/3}\,\mathrm{DEV}_{n+1}[\gamma \Pi_{n+1} + (1-\gamma)\bar{H}_{n+1}]\,. \tag{3.6}$$

Finally, the deviator $\mathrm{dev}\,\tau := \tau - \frac{1}{3}(\mathrm{tr}\,\tau)\mathbf{1}$ of the Kirchhoff stress tensor is obtained by transforming (3.6) to the current configuration as

$$\mathrm{dev}[\tau_{n+1}] = F_{n+1}\{\mathrm{DEV}_{n+1}[S_{n+1}]\}F_{n+1}^{t}\,. \tag{3.7}$$

REMARK 3.1. Note that the entire update procedure takes place in the reference configuration. Hence, objectivity of the algorithm with respect to superposed rigid-body motions onto the current configuration follows trivially. Further, note that the algorithm is second-order accurate.

REMARK 3.2. In the update procedure discussed above, only the stress deviator is involved. It remains to compute the hydrostatic pressure $p = \mathrm{d}U^0(J)/\mathrm{d}J$. We recall, however, that in a discrete sense the pressure constitutive equation cannot be enforced pointwise. This would lead to "locking" of the finite element procedure for quasi-incompressible response. To avoid these difficulties, the Jacobian J and the pressure p are interpolated independently in the context of a Hu–Washizu principle. This is considered in the next section.

3.2. *Consistent linearization of the algorithm*

By contrast with algorithms based on the notion of the midpoint configuration, the proposed approach can be exactly linearized in closed form. The resulting tangent moduli play a crucial role in the numerical solution of the boundary value problem by Newton-type iterative methods. For instance, use of these consistently linearized moduli is essential in order to preserve the quadratic rate of the asymptotic convergence that characterizes Newton's method.

We recall that at time step $t_{n+1} \in \mathbb{R}_+$ the material and spatial tangent moduli associated with the configuration $x_{n+1} = \varphi_{n+1}(X, t_{n+1})$, denoted by L_{n+1} and c_{n+1}, respectively, are defined in component form by

$$L_{n+1}^{IJKL} := \frac{\partial S^{IJ}}{\partial E^{KL}}\bigg|_{n+1}, \qquad c_{n+1}^{ijkl} = \left[\frac{1}{J}F_I^i F_J^j F_K^k F_L^l L^{IJKL}\right]_{n+1}. \tag{3.8a, b}$$

Since $S_{n+1} = \{JpC^{-1} + \mathrm{DEV}[S]\}_{n+1}$, differentiation of this expression yields the result

$$L_{n+1} \equiv \left[JC^{-1}\otimes\frac{\partial p}{\partial E}\right]_{n+1} + [Jp(C^{-1}\otimes C^{-1} - 2I_{C^{-1}}) + L_{\mathrm{dev}}]_{n+1}\,, \tag{3.9}$$

where $I_{C^{-1}}^{IJKL} := \frac{1}{2}[(C^{-1})^{IK}(C^{-1})^{JL} + (C^{-1})^{IL}(C^{-1})^{JK}]$, and L_{dev} is defined as

$$L_{\mathrm{dev}}\Big|_{n+1} := \frac{\partial(\mathrm{DEV}[S])}{\partial E}\bigg|_{n+1}. \tag{3.10}$$

Note that by (3.8b), the spatial counterpart of (3.9) is given by

$$\boldsymbol{c}_{n+1} := \left[\mathbf{1}\otimes\boldsymbol{F}\,\frac{\partial p}{\partial \boldsymbol{E}}\,\boldsymbol{F}^{t}\right]_{n+1} + [\,p(\mathbf{1}\otimes\mathbf{1} - 2\boldsymbol{I}) + \boldsymbol{c}_{\mathrm{dev}}]_{n+1}\,, \tag{3.11}$$

where $\boldsymbol{I}$ is the symmetric rank-four unit tensor, and $\boldsymbol{c}_{\mathrm{dev}}$ is defined in terms of $\boldsymbol{L}_{\mathrm{dev}}$ by a transformation (push-forward) identical to (3.8b). Thus, all that remains is to compute $\boldsymbol{L}_{\mathrm{dev}}$ or $\boldsymbol{c}_{\mathrm{dev}}$ by consistent linearization of the integration algorithm in Section 3.1.

As an illustration, we consider again the constitutive model outlined in Example 2.4 above. The main steps in the evaluation of $\boldsymbol{c}_{\mathrm{dev}}$ involve the repeated use of the directional derivative formula, and details are omitted. In order to express the final result in a compact form it is useful to define the rank-four spatial symmetric tensor $\mathrm{dev}[\bar{\boldsymbol{c}}]$ as follows. For notational simplicity, the subindex $n+1$ is omitted and all the expressions that follow are understood to be evaluated at t_{n+1}. Let

$$\bar{\boldsymbol{L}}^{0} := \partial^{2}\bar{\boldsymbol{\Psi}}^{0}(\bar{\boldsymbol{E}})/\partial\bar{\boldsymbol{E}}^{2}\,, \qquad [\bar{c}^{0}]^{ijkl} = \frac{1}{J}\,F^{i}_{I}F^{j}_{J}F^{k}_{K}F^{l}_{L}[\bar{L}^{0}]^{IJKL}\,. \tag{3.12}$$

Define $\mathrm{dev}[\bar{\boldsymbol{c}}^{0}]$ by the expression

$$\mathrm{dev}[\bar{\boldsymbol{c}}^{0}] := \boldsymbol{c}^{0} - \tfrac{1}{3}\,\mathbf{1}\otimes[\bar{\boldsymbol{c}}^{0}:\mathbf{1}] - \tfrac{1}{3}\,[\bar{\boldsymbol{c}}^{0}:\mathbf{1}]\otimes\mathbf{1} + \tfrac{1}{9}[\mathbf{1}:\bar{\boldsymbol{c}}^{0}:\mathbf{1}]\mathbf{1}\otimes\mathbf{1}\,. \tag{3.13}$$

With this notation at hand, the consistent tangent moduli $\boldsymbol{c}_{\mathrm{dev}}$ may be expressed as

$$\begin{aligned}(\det\boldsymbol{F})\boldsymbol{c}_{\mathrm{dev}} = {} & \tfrac{2}{3}\,\mathrm{tr}(\bar{\boldsymbol{h}} + \mu(\Delta t/\nu)\bar{\pi})\,[\boldsymbol{I} - \tfrac{1}{3}\mathbf{1}\otimes\mathbf{1}] - \tfrac{2}{3}[\bar{\pi}\otimes\mathbf{1} + \mathbf{1}\otimes\bar{\pi}] \\ & + (\det\boldsymbol{F})\mu(\Delta t/\nu)\bar{g}\,\mathrm{dev}[\bar{\boldsymbol{c}}^{0}] - \bar{g}'\,\frac{(\det\boldsymbol{F})^{2/3}}{\boldsymbol{\Xi}^{\mathrm{m}}\bar{g}}\,[\bar{\pi}\otimes\bar{\pi}]\,.\end{aligned} \tag{3.14}$$

In this expression, $\boldsymbol{I}$ is the rank-four unit tensor, $\mathbf{1}$ the rank-two unit tensor, and the following additional notation has been employed:

$$\bar{\boldsymbol{h}} = \bar{\boldsymbol{F}}\{\gamma\boldsymbol{\Pi} + (1-\gamma)\bar{\boldsymbol{H}}\}\bar{\boldsymbol{F}}^{t}\,, \qquad \bar{\pi} = \bar{\boldsymbol{F}}\boldsymbol{\Pi}\bar{\boldsymbol{F}}^{t}\,, \tag{3.15}$$

$$\mu(\Delta t/\nu) := \gamma + (1-\gamma)\,\frac{1 - \mathrm{e}^{\Delta t/\nu}}{\Delta t/\nu}\,.$$

Note that the moduli in (3.12) are symmetric.

4. Mixed variational formulation

We shall outline the variational framework for the numerical solution of the nonlinear boundary value problem by a mixed finite element formulation. The basic idea is to introduce a three-field variational formulation involving configuration, Jacobian, and pressure, $\{\boldsymbol{\varphi}, J, p\}$. The well-known locking phenomenon associated with overconstraining of displacement formulations may then be avoided by appropriate independent interpolation of the pressure and volume (Jacobian) fields.

Ignoring for simplicity inertia effects, the equilibrium of the body at each time step $t_{n+1} \in \mathbb{R}_+$ may be expressed as follows:

$$
\begin{aligned}
G_{n+1} &:= \int_{\varphi_{n+1}(\Omega)} \{ p_{n+1} \operatorname{div}_{n+1} \boldsymbol{\eta} + \operatorname{dev}[\boldsymbol{\sigma}_{n+1}] : \operatorname{dev}[\nabla_{n+1} \boldsymbol{\eta}] \} \, dv - G^{\mathrm{EXT}}_{n+1} = 0 , \\
\Gamma_{n+1} &:= \int_{\Omega} (\det \boldsymbol{F}_{n+1} - J_{n+1}) \delta p \, dV = 0 , \\
H_{n+1} &:= \int_{\Omega} \left\{ -p_{n+1} + \left. \frac{dU(J)}{dJ} \right|_{n+1} \right\} \delta J \, dV = 0 .
\end{aligned}
\tag{4.1}
$$

Here, $\boldsymbol{\eta}(\boldsymbol{x})$ are admissible variations satisfying the homogeneous essential boundary conditions, and G^{EXT}_{n+1} is the virtual work of the external loading, see e.g. [33, Section 5.1]. For nonlinear elasticity, these variational equations emanate from a nonlinear Hu–Washizu principle [45]. Note the crucial role played by the constitutive algorithm developed in Section 3 in this variational procedure. At time t_{n+1} the values of p_{n+1} and dev $[\boldsymbol{\sigma}_{n+1}]$ are known and computed through this algorithm.

The finite element numerical solution of variational equations (4.1) involves the projection of these equations onto a finite dimensional subspace. Conceptually, an iterative solution procedure is based on the following linearized system about an intermediate configuration $\{\boldsymbol{\varphi}^{(i)}_{n+1}, p^{(i)}_{n+1}, J^{(i)}_{n+1}\}$:

$$
\begin{aligned}
DG := & \begin{Bmatrix} G_{n+1} \\ \Gamma_{n+1} \\ H_{n+1} \end{Bmatrix}^{(i)} \\
& + \int_{\varphi^{(i)}_{n+1}(\Omega)} [\nabla \boldsymbol{\eta}, \delta p, \delta J] : \begin{bmatrix} \boldsymbol{a}^{I(i)}_{n+1} & \mathbf{1} & \mathbf{0} \\ \mathbf{1}^{\mathrm{t}} & 0 & -\dfrac{1}{\det \boldsymbol{F}^{(i)}_{n+1}} \\ \mathbf{0}^{\mathrm{t}} & -\dfrac{1}{\det \boldsymbol{F}^{(i)}_{n+1}} & \dfrac{U''}{\det \boldsymbol{F}^{(i)}_{n+1}} \end{bmatrix} \begin{Bmatrix} \nabla \boldsymbol{u} \\ \Delta p \\ \Delta J \end{Bmatrix} dv .
\end{aligned}
\tag{4.2}
$$

The moduli $\boldsymbol{a}^{(i)}_{n+1}$ appearing in the linearized equations (4.2) are defined according to the relation

$$
\nabla \boldsymbol{\eta} : \boldsymbol{a} : \nabla \boldsymbol{u} := \nabla \boldsymbol{\eta} : [\boldsymbol{\sigma} \nabla \boldsymbol{u}] + \nabla \boldsymbol{\eta} : [p(\mathbf{1} \otimes \mathbf{1} - 2\boldsymbol{I}) + \boldsymbol{c}_{\mathrm{dev}}] : \nabla \boldsymbol{u} ,
\tag{4.3}
$$

where, for notational simplicity, the subindex $n + 1$ and superindex (i) have been omitted. In this expression, $\boldsymbol{c}_{\mathrm{dev}}$ are the consistent tangent moduli defined, for Example 2.4, by (3.14). In a finite element context, the first term in (4.3) gives rise to the so-called "geometric stiffness" matrix, whereas the second term in (4.3) leads to the often referred to as material part of the tangent stiffness matrix.

Several finite element interpolations schemes can be used within the mixed variational framework provided by (4.1)–(4.2). As an example, discontinous pressure and Jacobian interpolations enable one to eliminate these fields at the element level leading to a generalized displacement method. Typical examples are furnished by the "mean dilatation" approach

suggested by Nagtegaal, Parks and Rice [32], and the B-bar methods of Hughes [20] and Simo et al. [45]. We refer to [35] for a summary account of existing mathematical results in the context of the linear problem.

5. Examples and numerical simulation

In this section, two experimental results corresponding to highly filled rubbers subject to extension and simple shear test are first considered. These results illustrate the good qualitative agreement obtained with the simple exponential damage law proposed in (2.10). Next, a simple numerical simulation is presented for the purpose of exhibiting the basic behavior of the viscoelastic damage model. Finally, the numerical solution of a boundary value problem is considered to illustrate the good performance of the integration algorithm, and the excellent convergence properties of the solution procedure.

EXAMPLE 5.1. In this example, we illustrate the ability of the exponential damage law (2.9) of modeling the qualitative response of highly filled rubbers. For this purpose, we consider first experimental data of a cyclic tension test performed at LLNL, and plotted in Fig. 1(a). Points in this figure correspond to measurements performed once steady state is achieved for a given double strain amplitude. The figure clearly exhibits a progressive degradation of the loss and storage moduli, denoted by G'' and G', respectively, with increasing amplitude. Figure

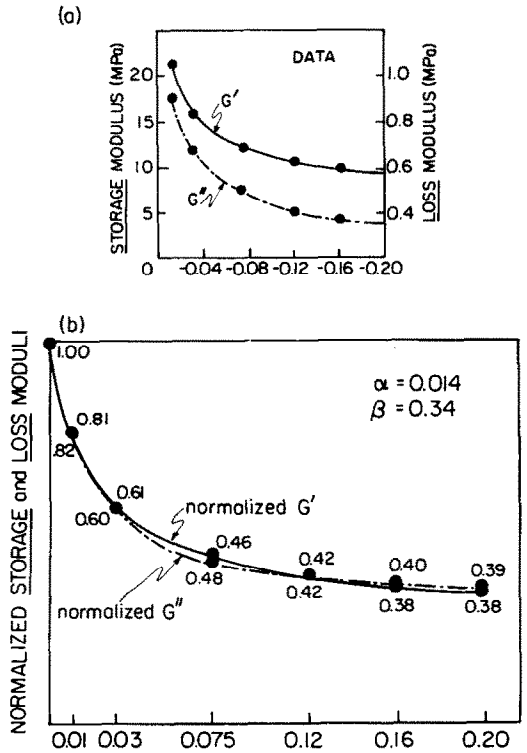

Fig. 1. Exponential fit to LLNL experimental data.

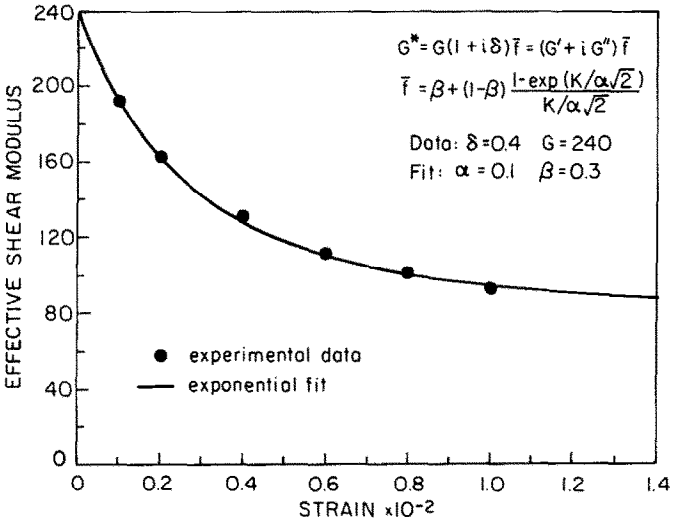

Fig. 2. Exponential fit to experimental data reported in [23]. The elastomer is a highly filled rubber.

1(b) shows the normalized curves obtained from Fig. 1(a). It is interesting to observe that the curves for G' and G'' in Fig. 1(a) lead to the same normalized curve in Fig. 1(b). This figure also exhibits the excellent fit obtained with the simple exponential damage law (2.10).

Figure 2 corresponds to the experimental data in simple shear reported by Kelly and Celebi [23]. In this figure, the fit obtained by means of the exponential damage law is also shown. Good agreement is again obtained.

EXAMPLE 5.2. In this example we consider the numerical simulation of a rubber block undergoing pure shear deformation. The data for this simulation corresponds to Fig. 2. The specimen is subjected to a cyclic shear strain history in the form of a triangular pulse, with increasing amplitude denoted by A. We have employed the notation: $G_\infty := \gamma\mu^0$ and $G_0 := (1-\gamma)\mu^0$.

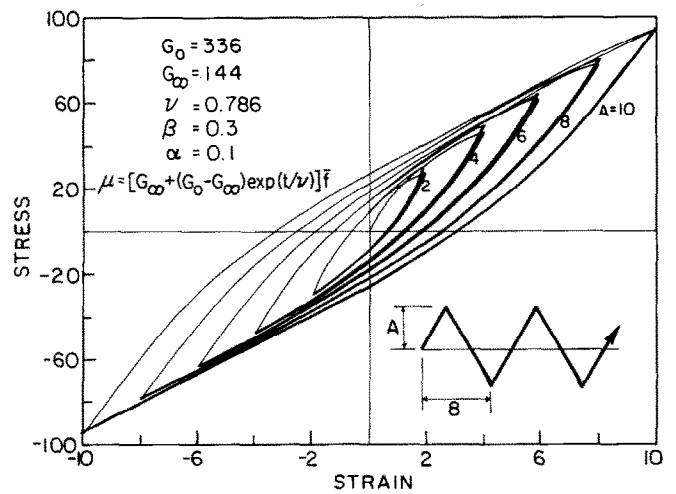

Fig. 3. Numerical simulation in a pure shear test with data obtained from Fig. 2. The strain history is a *triangular* pulse.

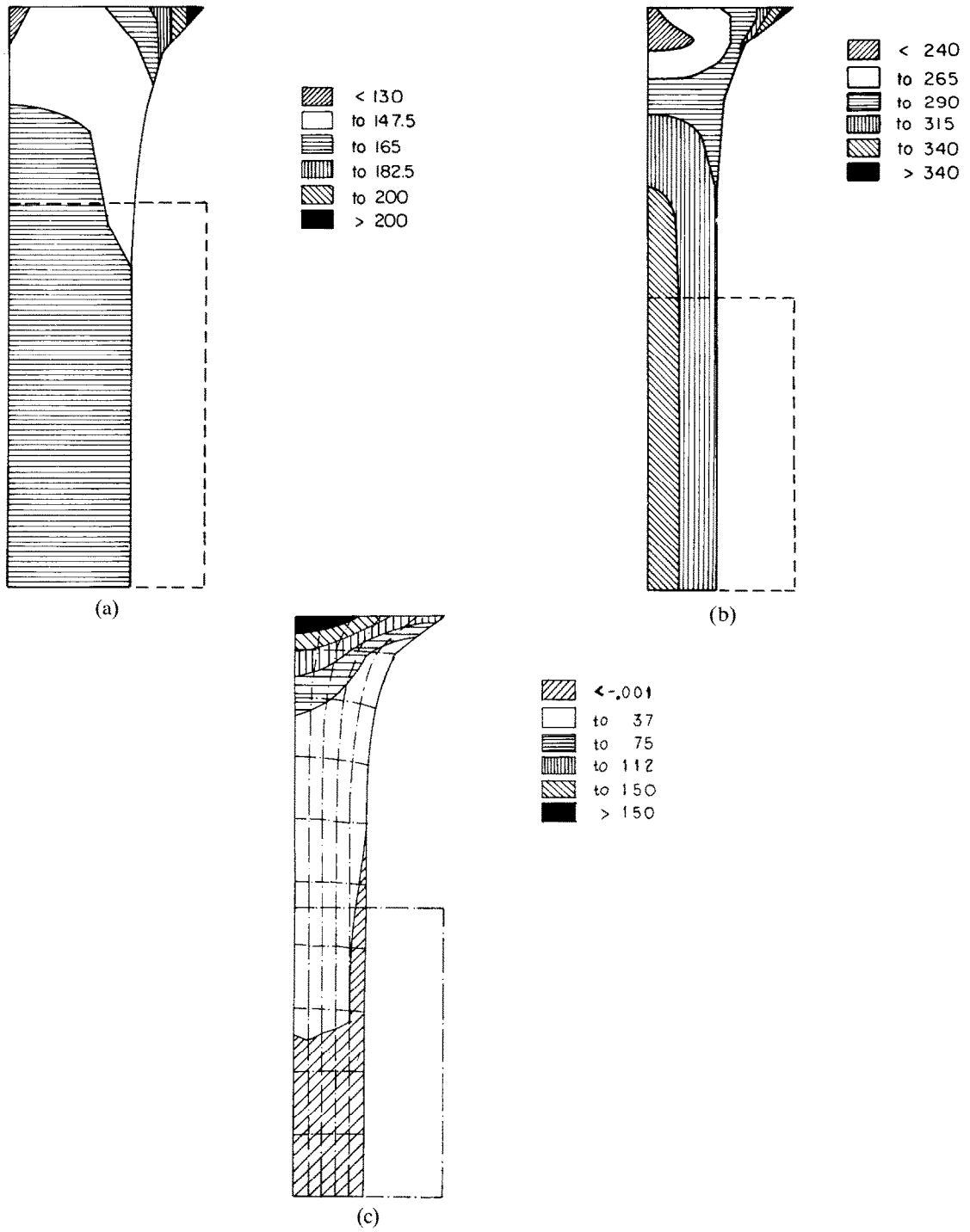

Fig. 4. Viscoelastic damage model. (a) 50% deformation. Contours of principal tensile stresses. 50 bilinear isoparametric quadrilateral elements with constant pressure. (b) 100% deformation. Clamped-clamped tensile test. Contours of principal stresses. 50 bilinear isoparametric quadrilateral elements with constant pressure. (c) 100% deformation. Clamped-clamped tensile test. Contours of principal (compressive) stresses. Deformed mesh also shown in the figure in dotted line.

The numerical results shown in Fig. 3 are in agreement with the experimental results reported in [23]. Although the stresses corresponding to peak strains are well captured, a discrepancy with the experimental results in the shape of the hysteresis loop is observed. This is attributed to the difference in shape of the pulse employed in the experimental test and in the numerical simulation. Identical simulations carried out with a sinusoidal pulse revealed the high sensitivity of the shape of the hysteresis loop to the shape of the input pulse.

EXAMPLE 5.3. As our final example, the numerical solution of the boundary value problem corresponding to the extension of a rectangular strip in plane strain clamped on both ends. The purpose of this simulation is to demonstrate the effectiveness of the numerical algorithm and finite element implementation discussed in Sections 3 and 4. We consider the viscoelastic damage model summarized in (2.14), with deviatoric stored energy $\bar{\Psi}^0(\boldsymbol{E})$ given by (1.14); that is, of the compressible neo-Hookean type. In addition, we assume that the hydrostatic pressure is given by the elastic constitutive equation $p = K \log J$, where $K > 0$ is the bulk modulus. The data for this example is contained in Fig. 3 with a value of α now chosen as $\alpha = 0.3333$. The finite element mesh consists of 50 bilinear four-noded isoparametric elements with constant Jacobian and constant pressure on the element in its *current* configuration. The deformed meshes and stress contours for principal stresses are shown in Figs. 4(a), (b) and (c) for extension ratios of 50% and 100%.

Special attention is given to the convergence behavior observed during the numerical simulation. The solution strategy employed is a standard Newton–Raphson solution procedure. The values of the maximum Euclidean norm of the out of balance force during the iteration process corresponding to loading steps 2, 3, and 4 are displayed in Table 1. We note that the final 100% extension was achieved in 6 loading steps. It should be also noted that the maximum norm is far more demanding than the usually employed energy norm. The results in Table 1 clearly demonstrate the quadratic behavior of the asymptotic rate of convergence.

Table 1
Values of the Euclidean norm of the residual

Step number	Maximum norm
2	$0.3941 \cdot 10^{5}$
	$0.6506 \cdot 10^{3}$
	$0.8008 \cdot 10^{2}$
	$0.2486 \cdot 10^{1}$
	$0.4285 \cdot 10^{-2}$
	$0.3705 \cdot 10^{-8}$
3	$0.3746 \cdot 10^{5}$
	$0.6159 \cdot 10^{3}$
	$0.2552 \cdot 10^{2}$
	$0.2526 \cdot 10^{1}$
	$0.4138 \cdot 10^{-3}$
	$0.2794 \cdot 10^{-9}$
4	$0.3591 \cdot 10^{5}$
	$0.5584 \cdot 10^{3}$
	$0.1005 \cdot 10^{2}$
	$0.4546 \cdot 10^{0}$
	$0.7936 \cdot 10^{-5}$

6. Closure

We have developed a fully nonlinear viscoelastic constitutive model capable of accommodating general anisotropic response and general relaxation functions. Complete uncoupling between volumetric and deviatoric responses may be achieved as a result of a multiplicative split of the deformation gradient into volumetric and deviatoric parts. Hyperelastic behavior is asymptotically obtained for both very fast and very slow processes. In addition, a simple isotropic damage mechanism has been incorporated into the model within the framework of continuum damage mechanics. Based on thermodynamic considerations, damage is characterized by the maximum value previously attained by the strain energy of the undamaged material. In a cyclic test, the resulting *viscoelastic damage model* predicts progressive loss of stiffness and increasing dissipation with increasing maximum amplitude, in agreement with Mullins' effect. Crucial to these developments is the assumed structure of the free energy potential, leading to an additive split of the stress tensor into initial and nonequilibrium parts.

Emphasis has been placed on the numerical treatment of the proposed formulation in the context of the finite element method. We have developed an implicit second-order accurate integration algorithm, which bypasses the need for the midpoint configurations, and trivially satisfies objectivity requirements under superposed rigid-body motions. This algorithm can be linearized exactly in closed form. Quasi-incompressible response has been numerically accounted for by means of a three-field variational formulation of the Hu–Washizu type.

Acknowledgment

The author is indebted to J. Lubliner and R.L. Taylor for helpful discussions. Partial support for this research was provided by a grant from the Lawrence Livermore National Laboratory.

References

[1] P.J. Blatz and W.L. Ko, Application of finite elastic theory to the deformation of rubbery materials, Trans. Soc. Rheology 6 (1968) 223–251.
[2] B. Bernstein, E.A. Kearsley and L.J. Zapas, Trans. Soc. Rheology 7 (1963) 391–410.
[3] B. Bernstein, E.A. Kearsley and L.J. Zapas, J. Res. Nat. Bur. Standards 68B (1964) 103.
[4] R.V. Browning, M.E. Gurtin and W.O. Williams, A viscoplastic constitutive theory for filled polymers, Internat. J. Solids and Structures 20 (11/12) (1983) 921–934.
[5] J.L. Chaboche, Continuous damage mechanics—A tool to describe phenomena before crack initiation, Nucl. Engrg. Design 64 (1981) 233–247.
[6] J.L. Chaboche, Le concept de contrainte effective appliqué à l'élasticité et à la viscoplasticité en présence d'un endommagement anisotrope, in: J.P. Boehler, ed., Mechanical Behavior of Anisotropic Solids, Proceedings EUROMECH Colloque 115 (Martinus Nijhoff, Leyden, The Netherlands, 1982) 737–760.
[7] R.M. Christensen, A nonlinear theory of viscoelasticity for application to elastomers, J. Appl. Mech. 47 (1980) 762–768.
[8] R.M. Christensen, Theory of Viscoelasticity: An Introduction (Academic Press, New York, 1971).
[9] B.D. Coleman and M. Gurtin, Thermodynamics with internal variables, J. Chem. Phys. 47 (1967) 597–613.
[10] R.J. Farris, The stress-strain behavior of mechanically degradable polymers, in: A.J. Chompff and S. Newman, eds., Polymer Networks: Structural and Mechanical Properties (Plenum, New York, 1971).

[11] J.D. Ferry, Viscoelastic Properties of Polymers (Wiley, New York, 2nd ed., 1970).
[12] R.J. Flory, Thermodynamic relations for high elastic materials, Trans. Faraday Soc. 57 (1961) 829–838.
[13] M. Fortin and R. Glowinski, Méthodes de Lagrangien augmenté. Application à la résolution numérique de problèmes aux limites (Dunod-Bordas, Paris, 1982).
[14] A.N. Gent, The Mechanics of Fracture, AMD 19 (ASME, New York, 1976) 55.
[15] M.S. Green and A.V. Tobolsky, A new approach to the theory of relaxing polymeric media, J. Phys. Chem. 14 (1946) 80–92.
[16] R. Glowinski, Numerical Methods for Nonlinear Variational Problems (Springer, Berlin, 1984).
[17] M.E. Gurtin and E.C. Francis, Simple rate-independent model for damage, J. Spacecraft 18 (3) (1981) 285–286.
[18] J.O. Hallquist, NIKE 2D: An implicit, finite deformation, finite element code for analyzing the static and dynamic response of two-dimensional solids, Rept. UCRL-52678, Lawrence Livermore National Laboratory, University of California, Livermore, CA, 1984.
[19] L.R. Herrmann and F.E. Peterson, A numerical procedure for viscoelastic stress analysis, in: Proceedings 7th Meeting of ICRPG Mechanical Behavior Working Group, Orlando, FL, 1968.
[20] T.J.R. Hughes, Generalization of selective integration procedures to anisotropic and nonlinear media, Internat. J. Numer. Meths. Engrg. 15 (9) (1980) 1413–1418.
[21] T.J.R. Hughes and J. Winget, Finite rotation effects in numerical integration of rate constitutive equations arising in large-deformation analysis, Internat. J. Numer. Meths. Engrg. 15 (9) (1980) 1413–1418.
[22] L.M. Kachanov, Time of the rupture process under creep conditions, Izv. Akad. Nauks SSR Otd. Tech. Nauk (1958) 26–31.
[23] J.M. Kelly and M.. Celebi, Verification testing of prototype bearings for based isolated building, Rept. No. UCB/SESM-84101, Department of Civil Engineering, University of California, Berkeley, CA, 1984.
[24] S.W. Key and R.D. Krieg, On the numerical implementation of inelastic time dependent and time independent, finite strain constitutive equations in structural mechanics, Comput. Meths. Appl. Mech. Engrg. 33 (1982) 439–452.
[25] R.C. Koeller, Application of fractional calculus to the theory of viscoelasticity, J. Appl. Mech. 51 (2) (1984) 299–307.
[26] E.J. Kramer, Microscopic and molecular fundamentals of crazing, Adv. Polymer Sci. 52/53 (1983).
[27] J. Lemaitre, How to use damage mechanics, Nucl. Engrg. Design 80 (1984) 233–245.
[28] J. Lemaitre, A continuous damage mechanics model for ductile fracture, J. Engrg. Mater. Tech. 107 (1985) 83–89.
[29] H. Leaderman, Elastic properties of filamentous materials, The Textile Foundation, Washington, D.C., 1943.
[30] J. Lubliner, A model of rubber viscoelasticity, Mech. Res. Comm. 12 (1985) 93–99.
[31] P.M. Naghdi and J.A. Trapp, The significance of formulating plasticity theory with reference to loading surfaces in strain space, Internat. J. Engrg. Sci. 13 (1975) 785–797.
[32] J.C. Nagtegaal, D.M. Parks and J.R. Rice, On numerically accurate finite element solutions in the fully plastic range, Comput. Meths. Appl. Mech. Engrg. 4 (1974) 153–177.
[33] J.E. Marsden and T.J.R. Hughes, Mathematical Foundations of Elasticity (Prentice-Hall, Englewood-Cliffs, NJ, 1983).
[34] L. Mullins, Softening of rubber by deformation, Rubber Chem. Technol. 42 (1969) 339–362.
[35] J.T. Oden and G. Carey, Finite Elements Vol. IV. Mathematical Aspects (Prentice-Hall, Englewood-Cliffs, NJ, 1983).
[36] R.W. Ogden, Elastic deformations in rubberlike solids, in: H.G. Hopkins and M.J. Sewell, eds., Mechanics of Solids, the Rodney Hill 60th Anniversary Volume (1982) 499–537.
[37] R.W. Ogden, Nonlinear Elastic Deformations (Ellis Horwood, Chichester, U.K., 1984).
[38] P.M. Pinsky, M. Ortiz and K.S. Pister, Numerical integration of rate constitutive equations in finite deformation analysis, Comput. Meths. Appl. Mech. Engrg. 40 (1983) 137–158.
[39] A.C. Pipkin and T.G. Rogers, A non-linear integral representation for viscoelastic behavior, J. Mech. Phys. Solids 16 (1968) 59–72.
[40] Yu. N. Rabotnov, Elements of Hereditary Solid Mechanics (Mir, Moscow, 1980).
[41] R.A. Schapery, A theory of non-linear viscoelasticity based on irreversible thermodynamics, in: Proceedings 5th National Congress of Applied Mechanics (ASME, New York, 1966) 511–530.

[42] F. Sidoroff, Un modele viscoelastique non lineaire avec configuration intermediaire, J. Méc. 13 (1974) 679–713.
[43] J.C. Simo and R.L. Taylor, A simple three dimensional model accounting for damage effects, Rept. No. UCB/SESM/83-10, Department of Civil Engineering, University of California, Berkely, CA, 1983.
[44] J.C. Simo and R.L. Taylor, A three dimensional finite deformation viscoelastic model accounting for damage effects, Rept. No. UCB/SESM/85-2, Department of Civil Engineering, University of California, Berkeley, CA, 1985.
[45] J.C. Simo, R.L. Taylor and K.S. Pister, Variational and projection methods for the volume constraint in finite deformation elastoplasticity, Comput. Meths. Appl. Mech. Engrg. 51 (1985) 177–208.
[46] C. Truesdell and W. Noll, The Nonlinear Field Theories, Handbuch der Physik, Band III/3 (Springer, Berlin,
[47] L. Mullins and N.R. Tobin, Stress softenings in rubber vulcanizates, Part 1, J. Appl. Polymer Sci. 9 (1965) 2993–3010.
[48] J.A.C. Harwood, L. Mullins and A.R. Payne, Stress softenings in natural rubber vulcanizates, Part II, J. Appl. Polymer Sci. 9 (1965) 3011–3021.
[49] A.R. Payne, Dynamic properties of heat-treated butyl vulcanizates, J. Appl. Polymer Sci. 7 (1963) 873.